



**HAL**  
open science

## Long-range structuring of nanoparticles by mimicry of a cholesteric liquid crystal

Michel Mitov, Cristelle Portet, Christian Bourgerette, Etienne Snoeck, Marc Verelst

### ► To cite this version:

Michel Mitov, Cristelle Portet, Christian Bourgerette, Etienne Snoeck, Marc Verelst. Long-range structuring of nanoparticles by mimicry of a cholesteric liquid crystal. *Nature Materials*, 2002, 1 (4), pp.229-231. 10.1038/nmat772. hal-03588701

**HAL Id: hal-03588701**

**<https://hal.science/hal-03588701>**

Submitted on 11 Mar 2022

**HAL** is a multi-disciplinary open access archive for the deposit and dissemination of scientific research documents, whether they are published or not. The documents may come from teaching and research institutions in France or abroad, or from public or private research centers.

L'archive ouverte pluridisciplinaire **HAL**, est destinée au dépôt et à la diffusion de documents scientifiques de niveau recherche, publiés ou non, émanant des établissements d'enseignement et de recherche français ou étrangers, des laboratoires publics ou privés.

# Long-range structuring of nanoparticles by mimicry of a cholesteric liquid crystal

MICHEL MITOV\*, CRISTELLE PORTET, CHRISTIAN BOURGERETTE, ETIENNE SNOECK AND MARC VERELST

Centre d'Elaboration de Matériaux et d'Etudes Structurales, CNRS, BP 4347, 31055 Toulouse cedex 4, France

\*email: mitov@cemes.fr

Patterning nanoobjects is an exciting interdisciplinary research area in current materials science due to new optical and optoelectronic properties and the need to miniaturize electronic components<sup>1, 2</sup>. Many techniques have been developed for assembling nanoparticles into two- and three-dimensional arrays<sup>3</sup>. Most of studies involving liquid crystals as templates have dealt with colloidal particles and nematic and smectic phases<sup>4-11</sup>. Here we evidence for the first time the long-range ordering of nanoparticles assemblies which adopt the helical configuration of the cholesteric liquid crystalline phase. Due to glass-forming cholesterics, the investigation of nanostructures is made possible by transmission electron microscopy. The platinum nanoparticles form periodic ribbons which mimic the well-known fingerprint cholesteric texture. Surprisingly, the nanoparticles do not decorate the cholesteric texture but create a novel helical structure with a larger helical pitch. By varying the molar fraction of cholesterol-containing mesogen in the liquid crystal host, we show that the distance between the ribbons is directly correlated to the pitch. Therefore this inherent length scale becomes a simple control parameter to tune the structuring of nanoparticles. These results demonstrate the modularity of such an assembly process which provides a versatile route to new materials systems.

We used siloxane liquid crystal oligomers which are a class of side-chains polymers<sup>12</sup>. Two kinds of mesogens (liquid crystalline entities) are attached to the siloxane backbone : a chiral cholesterol-containing mesogen and an achiral one. These compounds have low glassy transition temperatures of about 50-60°C which depend on the molar ratio in chiral mesogens. They present a wide cholesteric mesophase up to 180-210°C and the isotropic phase above. The pitch of the helical structure depends on the molar ratio in chiral mesogens and fundamental optical properties of selective light reflection are associated to the existence of an helix<sup>13</sup>. Here we used as-called silicon-blue (SB) and silicon-red (SR) compounds with reflection wavelengths respectively equal to 450 and 675 nm.

SB was dissolved in chloroform with a concentration of 10 wt.%. A drop was deposited on a carbon-coated grid for transmission electron microscopy (TEM) investigations. The chloroform was evaporated at room temperature. The grid was annealed in an oven at 130°C during 16 hours to achieve the cholesteric organization. Due to the low glassy transition temperature a quenching was simply realized at 25°C by setting the grid on a metallic plate. The viscous film became a glassy solid film. TEM images showed an array of periodic bright and dark lines (Fig. 1.a). This as-called fingerprint texture is mainly the result of mass loss during irradiation by the electron beam which acts as an etching depending on the initial molecular orientation<sup>14, 15</sup>. The distance between two dark or bright lines is of the order of the half-pitch. From Fig. 1.a, the mean distance is about 148 nm (see the Supplementary Information). The molecular orientation in dark (bright) lines is parallel (perpendicular) to the picture plane. The helical axis is everywhere perpendicular to the lines.

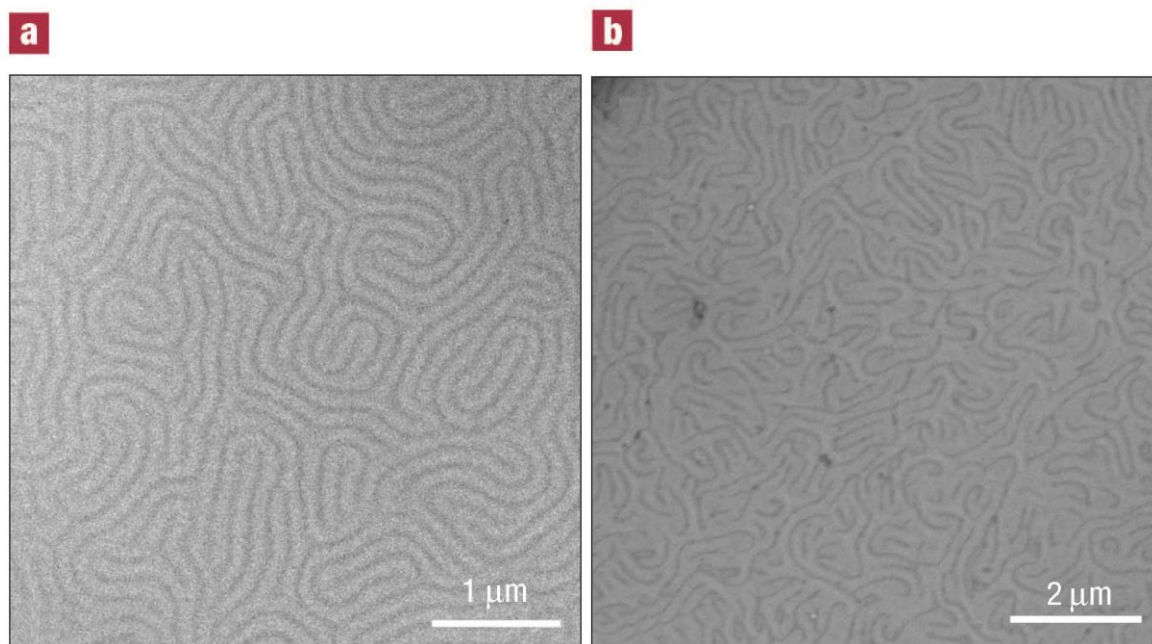


**Figure 1. Transmission electron micrographs of liquid crystalline materials. a,** TEM micrograph showing the fingerprint cholesteric texture for the pure liquid crystalline material. The distance between two dark or bright lines is of the order the half-pitch of the helical structure. Liquid crystalline molecules are preferentially parallel (perpendicular) to the picture plane in dark (bright) lines. The helical axis is everywhere perpendicular to the lines. **b,** TEM micrograph of cholesteric liquid crystal material now doped with nanoparticles (1.5 wt.%). Particle assemblies are structured into ribbons which mimic the fingerprint texture.

The nanoparticles we chose are platinum nanocrystals stabilized by one layer of a zwitterionic surfactant (sulfobetain, see the Supplementary Information). The particles were mixed with the previous solution with a concentration of 1.5 wt.% compared to the SB content. The blend was sonicated during 3 hours to favour the dispersion of particles. The preparation is then the same as for the pure liquid crystal film; at the end, the particles are embedded in a solid film in which the cholesteric order is stored. In an original way, TEM images showed periodic ribbons of nanoparticles assemblies which mimic the cholesteric fingerprint texture (Fig. 1.b). The distance between the

ribbons is about 225 nm. The ribbons are uniform in width and uniformly laid out in all the sample. The particles are significantly localized in the dark lines; as an equilibrium configuration, nanoparticles seem preferably fit into these parts, in which the orientation of liquid crystal molecules is preferentially parallel to the film plane, instead of into the bright lines.

A comparison can be usefully made between the assembly of platinum particles in the dark lines of the fingerprint texture and the physical principle of positive staining of polymers for electron microscopy investigation purposes<sup>16</sup>. The polymer sample is treated with heavy metal containing compounds such as osmium tetroxide  $\text{OsO}_4$  or ruthenium tetroxide  $\text{RuO}_4$  and peculiar regions are stained dark by either a chemical interaction or by a selective physical absorption of the staining agent inside the polymer film. In the latter case, and as an example, the longitudinal periodicity of nylon was revealed by the differential absorption of the staining agent (iodine) in the crystalline and noncrystalline regions<sup>17</sup>. In our case, and during the annealing process, the platinum nanoparticles can have preferably migrated in parts of the structured film containing the more free volume, hence a higher diffusion rate of particles in these regions corresponding to liquid crystalline elongated molecules which are lain down in the film plane and not perpendicular to it.

Inside a ribbon, the particles are disposed without any visible order (Fig. 2.a) and also without aggregation probably due to the presence of surfactant molecules grafted on the nanocrystal. The particles structuring does not only reflect the long-range ordering but also the topological constraints of the organized fluid; indeed, the assembling follows the well-known defects of the cholesteric phase called disclinations<sup>18</sup>. As an example, Figure 2.b shows like a  $\tau^+$ -type disclination in the ribbon distribution.

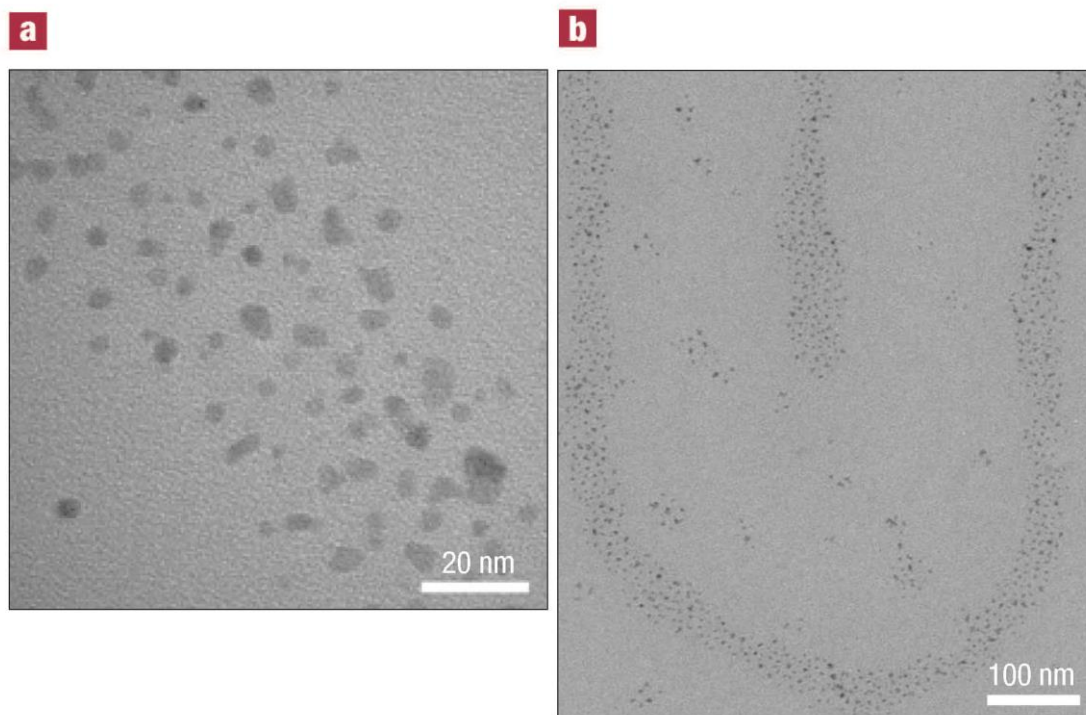


**Figure 2. Transmission electron micrographs of particles within ribbons. a,** Nanoparticles inside a ribbon. The particles are not aggregated. No ordering is visible. **b,** A particle ribbon organized into a typical cholesteric disclination ( $\tau^+$ -type). Thus the particles' structuring also reflect the topological constraints of the anisotropic fluid. Note that the area underlying the nanoparticles does not itself appear dark under high magnification.

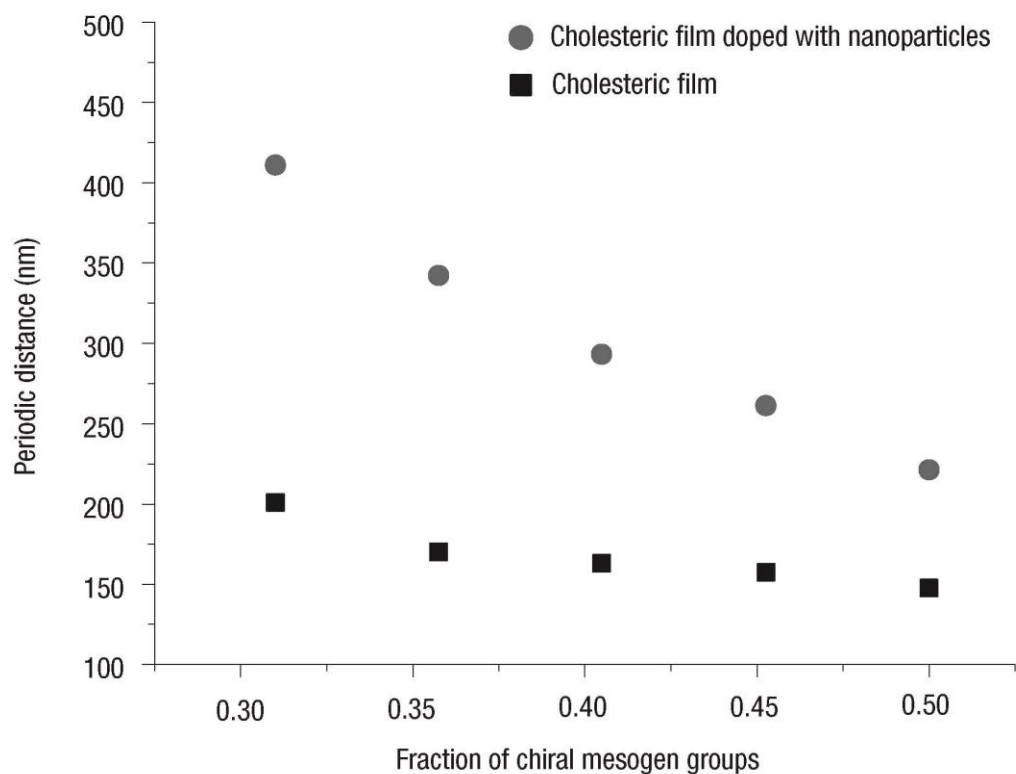


**Figure 3. Tuning the scale of the ‘fingerprint’.** The periodic distance between lines (ribbons) versus the molar fraction in chiral mesogens present in the pure (doped) cholesteric host. The particles lead to the formation of a novel helical structure with a larger pitch. The variation of structure periodicity for the doped material is correlated to the molecular chirality and hence to the helical pitch of the cholesteric liquid crystal. The pitch becomes a simple parameter for controlling the distance between particle ribbons.

To investigate the role of the inherent length scale such as the cholesteric periodicity on the structural characteristics of the auto-assembly, systematic changes in the chirality of the oligomer molecule, and hence in the helical pitch, were done. We chose different cases of cholesteric hosts : SB, SR and three intermediate blends (in wt.% : 75 of SB + 25 of SR, 50 of SB + 50 of SR and 25 of SB + 75 of SR). The variation of the periodic distance between lines and ribbons compared to the molar fraction in chiral mesogen is reported in Figure 3. The distance between two identical

lines decreases from about 200 to 150 nm when the molar fraction in cholesterol-containing mesogen in the cholesteric host increases from 31 to 50%. In parallel, for doped liquid crystalline materials with a constant concentration in nanoparticles of 1.5 wt.%, the distance between ribbons decreases from 410 to 225 nm. It is thus important to point out that the nanoparticles do not simply decorate the cholesteric texture but are intimately combined with the liquid crystal carrier; they experience specific interactions and create a novel helical structure with a larger pitch. For that reason, we think that the anisotropy of the nanoparticles assemblies is not simply due to a growth process in the fluid. Self-assembly depends critically on thermal energy; the resulting motion allows particles to attain the optimum positions to create the ordered structure. When the particles are smaller than the mesogens, the description in terms of elasticity is no longer relevant; the behaviour can be rather understood by considering entropic effects that are driven by hard core interactions between the mesogens and the particles<sup>5</sup>. Here the lengths of chiral and achiral mesogens are respectively equal to 26 and 19 Å and the size of nanoparticles (platinum core with the surfactant mantle) is about 62.5 Å; although the mesogens are two or three times smaller than the particle size, we may expect the understanding of the present self-assembly from entropic effects instead of the elasticity.

In a recent study, a planar array of one-dimensional chains of dodecanethiol-protected gold nanoparticles was fabricated by depositing the particles on a nanoscale ridge-and-valley structured carbon substrate<sup>19</sup>; the structures are likely to reflect the direction of valleys. In this approach, the particles organization comes from the periodic relief of the pre-chosen substrate whereas our self-assembly mechanism is the result of a true cooperative process during the annealing step as a compromise between the organisation of the anisotropic fluid and the presence of solid foreign particles. As stressed by the authors, most of chains have irregular spacings and nanoparticles are not arranged in a line; a regular array of chains was not obtained probably because the size



of particles (9.0 nm) is too large to sensitively distinguish between a ridge and a valley of carbon layer. By contrast, the arrangement of nanoparticles ribbons of our study is well-defined like being directly tuned by the choice of the helical pitch of the sustaining cholesteric matrix and the achievement of a well-organized texture. Additionally, the final one-dimensional array of gold particles is subjugated to the presence of a faceted surface whereas, by the very principle of our approach, the hybrid fluid could be deposited on various surfaces provided that the film presents a cholesteric organization (when necessary a surfactant layer could be deposited on the surface like in the case of liquid crystal displays).

This new type of hybrid system combines the long-range order of a cholesteric phase with the gas-like disorder of a suspension of particles. It allows one to address original questions concerning its structure, like the effect of solid particles on the true long-range helical order of liquid crystal molecules or reversibly the spatial arrangement of the nanoparticles confined inside one type of periodic lines present in the fingerprint texture. The fact that extended parallel ribbons of nanoparticles assemblies are formed with an interdistance correlated to the helical pitch illustrates the potential of our approach for the formation of various periodic structures.

## References

1. *Nanostructured Materials* (spec. iss. eds Bein, T. & Stucky, G. D.) *Chem. Mater.* **8**, 1569-2194 (1996).
2. Joachim, C., Gimzewski, J. K. & Aviram, A. Electronics using hybrid-molecular and mono-molecular devices *Nature* **408**, 541-548 (2000).
3. Pileni, M. P. Nanocrystal Self-Assemblies: Fabrication and Collective Properties *J. Phys. Chem. B* **105**, 3358-3371 (2001).

4. Poulin, P., Stark, H., Lubensky, T. C. & Weitz, D. A. Novel colloidal interactions in anisotropic fluids *Science* **275**, 1770-1773 (1997).
5. Poulin, P. Novel phases and colloidal assemblies in liquid crystals *Curr. Opinion in Colloid & Interf. Sci.* **4**, 66-71 (1999).
6. Fabre, P., Casagrande, C., Veyssié, M., Cabuil, V. & Massart, R. Ferrosmeectics: A New Magnetic and Mesomorphic Phase *Phys. Rev. Lett.* **64**, 539-542 (1990).
7. Burylov, S. V. & Raikher, Y. L. Orientation of a solid particle embedded in a monodomain nematic liquid crystal *Phys. Rev. E* **50**, 358-367 (1994).
8. Ponsinet, V. & Fabre, P. Flexibility of the membranes in a doped swollen lamellar phase *J. Phys. Chem.* **100**, 5035-5038 (1996).
9. Ramos, L., Fabre, P., Dubois, E. Compatibility between solid particles and a lamellar phase : a crucial role of the membrane interactions *J. Phys. Chem.* **100**, 4533-4537 (1996).
10. Sens, P., Turner, M. S. & Pincus, P. Particulate inclusions in lamellar phase *Phys. Rev. E* **55**, 4394-4405 (1997).
11. Poulin, P. & Weitz, D. A. Inverted and multiple nematic emulsions *Phys. Rev. E* **57**, 626-637 (1998).
12. Kreuzer, F.-H., Andrejewski, D., Haas, W., Häberle, N., Riepl, G. & Spes, P. Cyclic Siloxanes with Mesogenic Side Groups *Mol. Cryst. Liq. Cryst.* **199**, 345-378 (1991).
13. Kitzerow, H.-S. & Bahr, C. (eds.) *Chirality in Liquid Crystals* (Springer-Verlag, New-York, 2001).
14. Pierron, J., Boudet, A., Sopéna, P., Mitov, M. & Sixou, P. Cholesteric textures observed by transmission electron microscopy in diffraction contrast *Liq. Cryst.* **19**, 257-267 (1995).

15. Boudet, A., Mitov, M., Bourgerette, C., Ondarçuhu, T. & Coratger, R. Glassy cholesteric structure : thickness variation induced by electron radiation in transmission electron microscopy investigated by atomic force microscopy *Ultramicroscopy* **88**, 219-229 (2001).
16. Sawyer, L. C. & Grubb, D. T. in *Polymer Microscopy*, 93-109 (Chapman and Hall, London, 1987).
17. Hess, K. & Kiessig, H. Über Langperiodeninterferenzen und micellaren Faserfeinbau bei vollsynthetischen Fasern (Polyamide und Polyester) *Z. Physikal. Chem. A* **193**, 196-217 (1944).
18. Bouligand, Y. in *Physical Properties of Liquid Crystals* (Demus, D., Goodby, J., Gray, G. W., Spiess, H.-W. & Vill, V. eds.) 304-351 (Wiley-VCH, Weinheim, 1999).
19. Teranishi, T., Sugawara A., Shimizu, T. & Miyake, M. Planar Array of 1D Gold Nanoparticles on Ridge-and-Valley Structured Carbon *J. Am. Chem. Soc.* **124**, 4210-4211 (2002).

#### Acknowledgements

We thank Drs. F.-H. Kreuzer and E. Hanelt (Wacker Chemie GmbH) for having provided us with cholesteric liquid crystalline materials.

We thank C. Joachim for his fruitful remarks on the manuscript.

Correspondence and requests for materials should be addressed to M. M.

Supplementary Information accompanies the paper on the website for Nature Materials

(<http://www.nature.com/naturematerials>).

#### Competing financial interests

The authors declare that they have no competing financial interests.

Long-range structuring of nanoparticles by mimetism with a cholesteric liquid crystal

MICHEL MITOV, CRISTELLE PORTET, CHRISTIAN BOURGERETTE, ETIENNE SNOECK & MARC VERELST

SYNTHESIS AND ANALYSIS OF TEM MICROGRAPHS

Platinum nanoparticle synthesis.

Only analytic grade reagents were used for the synthesis, without any further purification. For the platinum (Pt) clusters elaboration, we reproduced the conditions reported by M. T. Reetz and W. Helbig for metallic nanoparticles synthesis (see *J. Am. Chem. Soc.* **1994**, *116*, 7401) but with a different geometry for the cell. Ours was composed of two concentric cylindrical Pt electrodes; the outer one (10 cm<sup>2</sup>) was the anode whereas the inner one (5 cm<sup>2</sup>) was the cathode. The cell was thermally regulated (25°C) by a double-wall vessel filled with water. A mechanical agitator passed through the cell by means of an airtight connection. The Pt clusters were synthesised via an electrochemical reaction using the sulphobetaine (C<sub>19</sub>H<sub>41</sub>NSO<sub>3</sub>) which is a zwitterionic surfactant (a zwitterionic molecule is globally non ionic but present a positively charged head N<sup>+</sup>R<sub>4</sub> and a negative one S<sup>-</sup>O<sub>3</sub>). The use of a zwitterionic surfactant leads to nanoparticles soluble in polar solvents (water, chloroform). 20 ml of water is added to the solution in order to increase the solution conductivity. The metal source was PtCl<sub>2</sub> (1500 mg) dissolved in THF (300 ml). 11 g is sulphobetaine amount (0.1 mol/l). The electrolysis was performed using a current density of 10 mA.cm<sup>-2</sup> during 45 h. The first untreated batch was obtained by complete solvent extraction of this solution. Then, the untreated batch was redissolved in absolute ethanol (200 ml) and left to settle during 2 h. A black powder was obtained by filtration. This operation is then renewed twice. This refinement procedure leads to almost monodispersed Pt nanoparticles stabilized only by one surfactant monolayer. Indeed, investigations by Scanning Tunneling Microscopy reveal the size of particles plus the protecting mantle (diameter = 6.25 nm, standard deviation = 1.10 nm), whereas the TEM images show only the metallic core (diameter = 3.35 nm, standard deviation = 0.45 nm). Thus, the thickness of the protecting mantle (6.25-3.35)/2 = 1.45 nm corresponds roughly to the size of one sulphobetaine molecule. Wide Angle X-Ray Scattering analysis shows that these nanoparticles have the classical fcc structure with cell parameter similar for bulky Pt.

Analysis of TEM micrographs and periodicity measurements.

The microstructure, size distribution and periodicity of the lines or ribbons were studied by TEM on a CM30 Philips microscope fitted with a 1024x1024 Gatan CCD camera at a magnification of about 1500 giving a resolution of 114 pixels/micron. The mean distance between the lines or ribbons has been determined computing the Fourier Transform (FT) of the TEM micrographs. The image analysis was performed using the SEMPER program on a UNIX environment. The power spectra of the FT evidence in the reciprocal space the main spatial frequencies appearing in the original images. Such a FT of the TEM image in Fig. 1a is reported in Fig. 4. The diffuse isotropic halo which surrounds the k<sub>0</sub> = 0 centre in the power spectrum indicates that there is no preferential direction of the lines at least over the whole TEM image (4.47 x 4.47 μm<sup>2</sup>). The position of the maximum of this diffuse ring was determined doing a profile of the reciprocal space in various directions and fitting the resulting curve in Fig. 4b by three Lorentz functions. The width of the ± k<sub>1</sub> peaks is related to the inverse of the dark/white fringes number (i.e. number of lines) in the original image (the less number of lines, the broadest peak) while their positions give the mean distance Δ between lines with the relation Δ = 2πA/k<sub>1</sub> (A is a constant depending on the digitised image size).

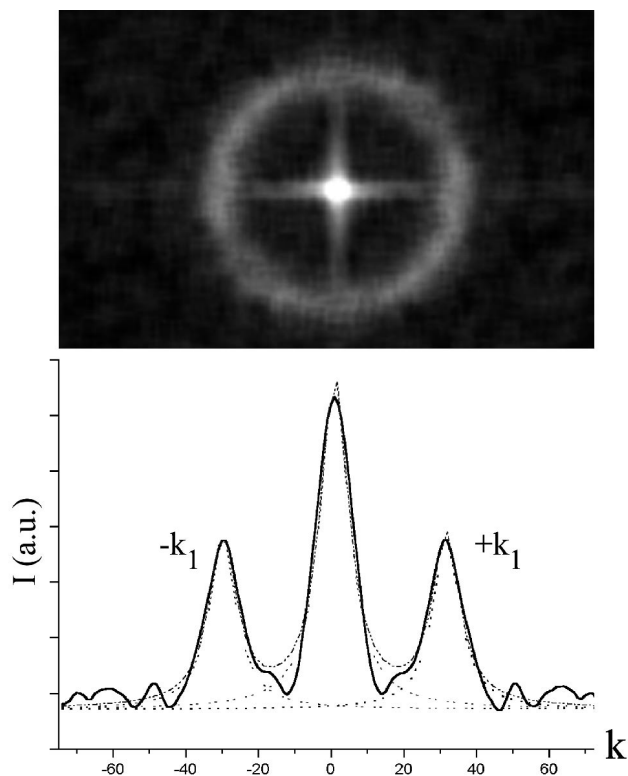


Figure 4 Fourier transform (FT) of the TEM image in Fig.1.a evidencing an isotropic diffuse ring around the main k=0 center, and profile of the FT allowing the precise determination of the ± k<sub>1</sub> position.